Optical nonlinearity in silicon nanoparticles: Effect of size and probing intensity

Sudakshina Prusty, H. S. Mavi,* and A. K. Shukla
Physics Department, Indian Institute of Technology, Hauz Khas, New Delhi 110016, India
(Received 2 September 2004; revised manuscript received 9 November 2004; published 31 March 2005)

Self-phase modulated optical fringe patterns are used to study the nonlinear optical response of nanocrystalline silicon produced by laser-induced etching. Intensity-dependent changes in the refractive index are calculated for various sizes of nanocrystallites. Raman spectroscopy is used to determine the sizes of nanocrystals, which are also confirmed from atomic force microscopic images. These results are in agreement with self-phase modulation model. It invokes the change in refractive index of nanoparticles of silicon with decrease of size of nanoparticles.

DOI: 10.1103/PhysRevB.71.113313 PACS number(s): 78.20.−e, 78.30.Am, 63.22.+m

The nanoparticles of silicon (NS) are emerging as multifunctional materials having diverse applications. Besides their efficient photoluminescence at room temperature,[1] the nonlinear optical properties of the NS are of immense research interest in recent years owing to the enhanced third-order optical nonlinearity.[2–5] An enhancement in the third-order susceptibility and the change in refractive index due to quantum confinement effect have been reported for laser ablated Si nanoclusters,[2,4] free-standing porous silicon materials,[3] and Si nanocrystals grown by plasma-enhanced chemical vapor deposition.[5] The nonlinear coefficient of the refractive index for NS has been calculated at different wavelengths prepared by various fabrication methods. The large deviation in the data is mainly due to the inhomogeneity of the samples owing to various fabrication techniques and different size distributions. Thus, the dimension and the size distribution of the NS are extremely important factors in order to reveal the nonlinear optical properties. In most of the measurements of optical nonlinear studies, higher laser power and short pulse lasers have been used.[2–5] In our measurements we have measured nonlinear refractive index with a cw argon ion laser at a wavelength in visible range.

Laser-induced etching[6,7] (LIE) is one of the simplest techniques for fabricating the nanoparticles. Under carefully controlled experimental parameters, NS can be produced on a silicon substrate with a narrow size distribution within a short time span of few minutes. However, there are no reports of measurement of nonlinear refractive index of NS prepared by LIE. Since the NS are formed directly on the silicon substrate, it is not possible to obtain the nonlinear refractive index directly by *Z*-scan measurement of the transmitted light.

In our earlier work,[8] we have reported the formation of visible optical fringes during the fabrication of NS and formulated the radial nonlinear changes in the refractive index of the medium due to self phase modulation of light.[9] However, there is a need for a more specific and detailed study on the nonlinear optical properties of NS. It is generally believed that the quantum confinement enhances third-order electronic susceptibility $\chi^{(3)}$ compared to the value for bulk silicon.[10] A controlled production of silicon nanocrystallites particularly referring to the dimension and size distribution is thus essential to relate the nonlinear optical properties to the quantum-confinement effect.

Here, we present a detailed study of the interaction between incident light and NS as a function of size of the nanoparticles and the incident laser intensity. A theoretical model of self-phase modulation, which describes the changes in the refractive index for nanoparticles of Si taking into account the size of crystallites in the medium, is discussed here. We also present a systematic study of the optical fringe patterns with the size of the NS and the probing laser intensity. Consequently, the radial changes of the nonlinear refractive index across the beam can be calculated as a function of both the size and laser intensity. The sizes of the NS are estimated by Raman spectroscopy. The line-shape analysis of the first-order Raman spectrum of the quantum-confined phonons provides the average and the distribution of sizes of NS, using the phenomenological quantum-confinement model.[11–14] The particle sizes are also estimated using atomic

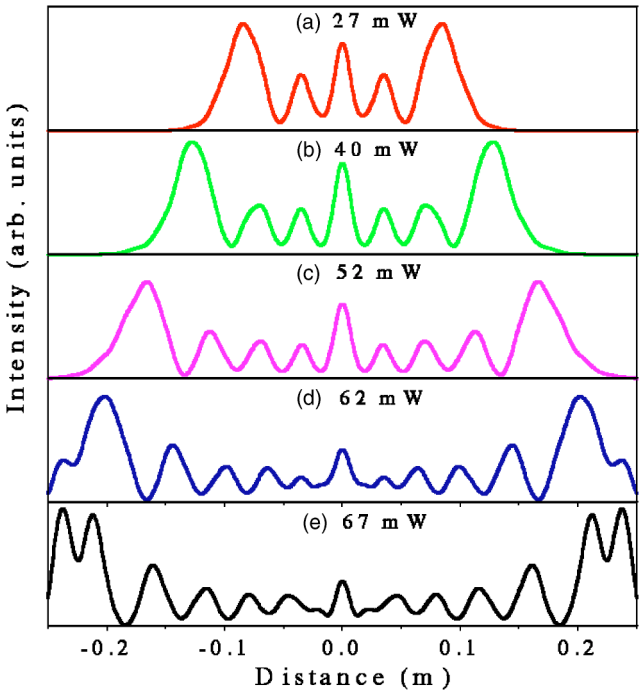

FIG. 1. (Color online) The theoretically calculated plot of fringe patterns using Eq. (2) of Ref. 8 for mean crystallite size, L_0=4 nm corresponding to different incident laser powers.

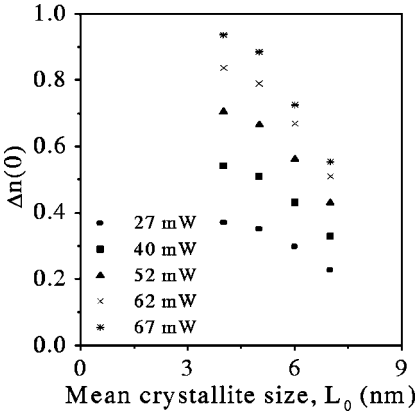

FIG. 2. The theoretically calculated changes in refractive index, $\Delta n(r)$, as a function of mean crystallite size, L_0, for different incident laser powers.

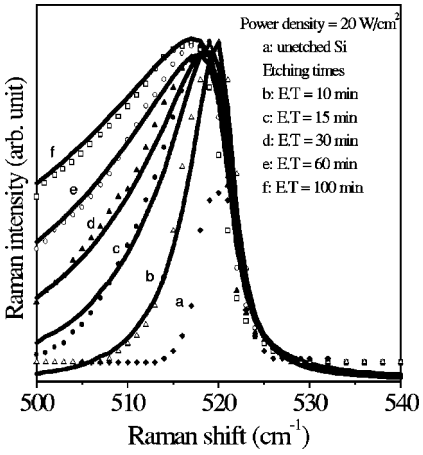

FIG. 3. The Raman spectra of Si etched for different times. The scattered points are the experimental data and the solid lines are the respective theoretical best fits using Eq. (3) of Ref. 15.

force microscope (AFM). We have calculated nonlinear changes in the refractive index for different sizes of nanocrystals. The experimental results of Raman scattering and nonlinear optical fringes are in agreement with our simple theoretical model.

A commercially available *n*-type Si wafer with resistivity of 10 Ω cm was immersed in HF acid (40%). LIE was done using an argon-ion laser ($\lambda = 5145$ Å). The laser beam was focused to a 100 μm spot and the laser power density used was 20 W/cm^2 during LIE. The samples were etched in this way for the durations of 10, 15, 30, 60, and 100 min. The laser-etched samples were subsequently rinsed with ethanol and were dried in air. During etching, the reflected beam was studied as the NS were formed on Si substrate. A white screen was placed at a distance 1.5 m from the surface of the crystal to observe the optical fringe patterns formed by the reflected beam in nearly back reflection geometry. Finally, the optical fringes formed for different incident laser powers were recorded by charge-coupled device (CCD) camera. Raman spectra were recorded for the etched samples. Details of the Raman spectroscopy system are given in Ref. 8. The recording of fringe patterns and the Raman spectra were repeated several times in order to ascertain their reproducibility. The AFM measurements were performed by using Digital Instruments Nanoscope in contact mode.

When an intense laser beam having a Gaussian profile, is incident on a medium containing nanocrystallites of Si, the refractive index of such material is altered by the intensity of the laser beam. As the nanocrystallites of Si interact with spatially varying laser intensity, the refractive index of the medium changes. Thus, the beam propagates in varied optical paths and hence there occurs spatial phase variation. This leads to a visible optical fringe pattern in the transverse plane and the phenomenon is known as spatial self-phase modulation.[9] The far-field diffraction intensity distribution of the optical fringe pattern has been discussed qualitatively in Eq. (2) of Ref. 8. The distribution of change in the refractive index of the medium containing nanocrystallites of silicon across the propagation of the beam, $\Delta n(r)$, is written as[8]

$$\Delta n(r) = \gamma_L I(r), \tag{1}$$

where γ_L is the nonlinear coefficient and $I(r)$ is the incident laser intensity. Here, we propose that γ_L depends on the size distribution of the nanoparticles and is not merely a constant for quantum-confined structures. Thus γ_L can be written as

$$\gamma_L = \int_{L_1}^{L_2} f \frac{N(L)}{L} dL, \tag{2}$$

where f is the coupling constant of light with the medium containing nanocrystallites and the integration takes care of the size distribution of the nanocrystallites. The $N(L)$ is the Gaussian distribution of nanocrystallites between L_1 and L_2, where L_1 and L_2 are the minimum and maximum sizes of the nanocrystallites. The theoretical plots of optical fringes for a

TABLE I. Calculated sizes of nanocrystallites for different irradiation times and the experimentally measured FWHM and Raman peak positions.

Irradiation time (min)	L_0 (Å)	L_1 (Å)	L_2 (Å)	σ (Å)	FWHM (cm^{-1})	Raman peak position (cm^{-1})
10	70	55	100	30	6.6	520
15	60	30	70	30	10.9	519
30	40	30	45	30	14.7	518
60	30	20	42	30	19	517.5
100	25	13	39	30	27.3	517

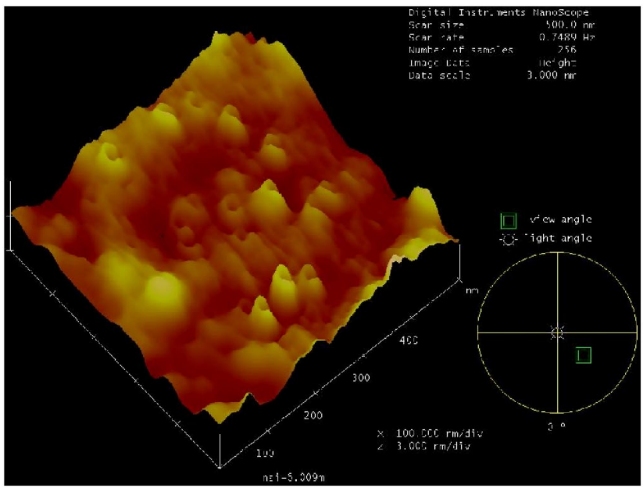

FIG. 4. (Color online) AFM picture of a laser-etched sample showing nanoparticles of Si.

particular mean crystallite size with different laser probing intensities are calculated using Eq. (2) of Ref. 8 and is displayed in Fig. 1. When the sizes of nanocrystallites are large, we do not observe any optical fringe pattern. The laser intensity on the sample is used as a parameter to assess the resulting nonlinear lensing effect. It shows that the number of optical fringes increases from 3 to 7 on increasing the probing laser intensity from 27 to 67 mW. We have also calculated theoretically a change in refractive index $[\Delta n(r)$ at $r=0]$ using Eq. (1) for different mean crystallite sizes (plotted in Fig. 2). To confirm the above results, we have recorded optical fringes with different laser intensities and Raman spectroscopy is used to determine the sizes of nanocrystallites (described below).

Figure 3 illustrates Raman spectra of the NS samples etched by an argon-ion laser for durations of 10, 15, 30, 60, and 100 min with laser power density of 20 W/cm^2. The changes in the Raman line shapes were very much apparent after the samples were etched for a minimum of 10 min. The FWHM (full width at half maximum) increases to 6.6 cm^{-1} as compared to the bulk value (3.5 cm^{-1}) without any change in the Raman peak position. On increasing the irradiation time the asymmetric broadening increases further and the Raman peak position is shifted to 517 cm^{-1} for 100 min of etching, as shown in Fig. 3. The size of nanocrystals can be determined by employing the phonon confinement model.[11–14] The details of size calculation are discussed in Ref. 15. It is determined by the two parameters L_0 and σ, where L_0 is the most probable or average size of the nanocrystals and σ defines the width of distribution. The calculated sizes for different etching times are listed in Table I for all Raman modes observed in Fig. 3. Figure 4 shows the AFM image of a laser-etched sample, which gives optical fringes. Nanoparticles of Si of height 1–5 nm are found on the surface. This result is consistent with the size determined by the Raman spectroscopy. Similar results were found for other laser-etched samples.

Figure 5 shows the photograph some of the optical fringe patterns observed experimentally with increasing intensity of the probing laser beam. The reflected beam from the sample

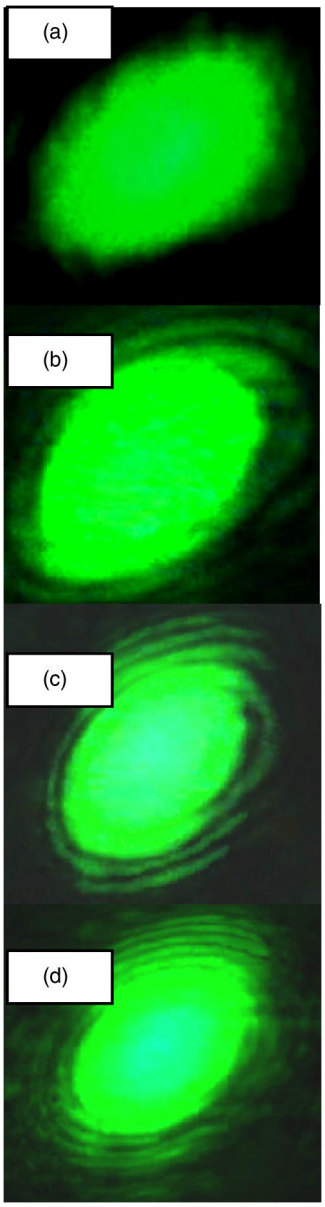

FIG. 5. (Color online) Photograph of fringe patterns at different incident laser powers: (a) 30 mW, just after irradiation and (b) 30 mW, (c) 50 mW, and (d) 70 mW, after 30 min of irradiation.

during etching was recorded by a CCD camera. Initially, at lower power an oval-shaped reflected spot is observed without any fringe patterns. As the intensity is increased gradually, the spot becomes brighter and a concentric fringe pattern is observed, as shown in Fig. 5. On increasing the laser power from 30 to 70 mW, the number of rings increases from 3 to 7. As the probing laser intensity increases, the refractive index changes resulting in the nonlinear phase variation across the incident laser beam. This leads to a change in the optical fringe pattern.

As we have discussed earlier, Eq. (1) can be used to calculate the changes in real refractive index at $r=0$. For a sample containing the nanoparticles prepared by laser-induced etching for an irradiation time of 30 min and incident power density of 20 W/cm^2, Raman spectroscopy pro-

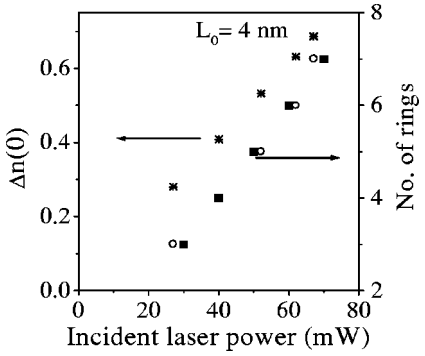

FIG. 6. The theoretically calculated maximum changes in refractive index, $\Delta n(r)$, (shown by stars) using Eq. (1). The corresponding theoretically obtained and experimentally observed number of rings (shown by open circles and solid squares, respectively) as a function of incident laser powers for mean crystallite size, $L_0=4$ nm.

vides the mean crystallite size, $L_0=40$, $L_1=30$, and $L_2=45$. Putting these values in Eq. (1), we have calculated the changes in real refractive index for different values of laser intensities $I(r)$ and are plotted in Fig. 6 (shown by stars). The enhancement of real refractive index is noticed here from 0.3 to 0.7 on increasing the laser power from about 30 to 70 mW. Correspondingly, the theoretically generated and experimentally observed number of rings are also plotted in Fig. 6 (shown by open circles and solid squares, respectively). This will also depend on nanocrystallite sizes and distributions. These data further emphasize that nonlinear phase arises across the beam on increasing laser power intensity for a particular mean crystallite size. Vijayalakshmi *et al.*[4] have also reported increase in refractive index (Δn) in laser ablated silicon nanostructures as high as 0.5.

On the whole, the nonlinear optical properties of Si nanoparticles formed by LIE were examined. The observed fringe patterns in Fig. 5 are the results from the nonlinear change in refractive index of the medium containing nanoparticles. We have attempted to correlate the nonlinear optical effect with both the incident laser intensity and the size of the nanoparticles. The magnitude of the nonlinear refractive index was found to increase linearly with increasing laser power for a particular size of nanoparticles. The value as high as 0.7 was calculated using self-phase modulation for the mean crystallite size of 4 nm. Thus the nonlinear effect can be the basis for the possible application of NS as an efficient material in nonlinear optical devices.

*Email address: hsmavi@physics.iitd.ernet.in

[1] L. T. Canham, Appl. Phys. Lett. **57**, 1046 (1990).
[2] S. Vijayalakshmi, M. A. George, and H. Grebel, Appl. Phys. Lett. **70**, 708 (1997).
[3] S. Lettieri, O. Fiore, P. Maddalena, D. Ninno, G. D. Francia, and V. La Ferrara, Opt. Commun. **168**, 383 (1999).
[4] S. Vijayalakshmi, A. Lan, Z. Iqbal, and H. Grebel, J. Appl. Phys. **92**, 2490 (2002).
[5] G. Vijayaprakash, M. Cazzanelli, Z. Gaburro, L. Pavesi, F. Iacona, G. Franzo, and F. Priolo, J. Appl. Phys. **91**, 4607 (2002).
[6] A. Starovoitov, S. Bayliss, Appl. Phys. Lett. **73**, 1284 (1998).
[7] M. L. Ngan, K. C. Lee, K. W. Cheah, J. Appl. Phys. **83**, 1637 (1998).
[8] H. S. Mavi, Sudakshina Prusty, A. K. Shukla, and S. C. Abbi, Opt. Commun. **226**, 405 (2003).
[9] Y. R. Shen, *The Principles of Nonlinear Optics* (Wiley, New York, 1984).
[10] S. Schmitt-Rink, D. A. B. Miller, and D. S. Chemla, Phys. Rev. B **35**, 8113 (1987).
[11] H. Richter, Z. P. Wang, L. Ley, Solid State Commun. **39**, 625 (1981).
[12] I. H. Campbell, P. M. Fauchet, Solid State Commun. **58**, 739 (1986).
[13] T. Suemoto, K. Tanaka, A. Nakajima, and T. Itakura, Phys. Rev. Lett. **70**, 3659 (1993).
[14] H. Yorikawa and S. Muramatsu, Appl. Phys. Lett. **71**, 644 (1997).
[15] B. G. Rasheed, H. S. Mavi, A. K. Shukla, S. C. Abbi, and K. P. Jain, Mater. Sci. Eng., B **79**, 71 (2001).